Phylloseptin-PBa1, -PBa2, -PBa3: Three novel antimicrobial peptides from the skin secretion of Burmeister's leaf frog (Phyllomedusa burmeisteri)

Wu, Y., Wang, L., Zhou, M., Chen, T., & Shaw, C. (2019). Phylloseptin-PBa1, -PBa2, -PBa3: Three novel antimicrobial peptides from the skin secretion of Burmeister's leaf frog (Phyllomedusa burmeisteri). *Biochemical and Biophysical Research Communications*. Advance online publication. https://doi.org/10.1016/j.bbrc.2018.12.156

Published in:
Biochemical and Biophysical Research Communications

Document Version:
Peer reviewed version

Phylloseptine-PBa1, -PBa2, -PBa3: Three novel antimicrobial peptides from the skin secretion of Burmeister's leaf frog (*Phyllomedusa burmeisteri*)

Youjia Wu [1,2*], Lei Wang [3], Mei Zhou [3], Tianbao Chen [3] and Chris Shaw [3]

1 Higher Educational Key Laboratory for Nano Biomedical Technology of Fujian Province, School of Pharmacy, Fujian Medical University, No.1 North Xuefu Road, 350108, Fuzhou, Fujian, China

2 Department of Pharmaceutical Analysis, School of Pharmacy, Fujian Medical University, No.1 North Xuefu Road, 350108, Fuzhou, Fujian, China

3 Natural Drug Discovery Group, School of Pharmacy, Queen's University Belfast, 97 Lisburn Road, BT9 7BL, Belfast, Northern Ireland, UK

* Correspondence: yoga0411@hotmail.com

Abstract

Skin secretions are known as a highly-complex mixture of abundant and diverse bioactive molecules and its study has attracted increasing attention over recent years. Phylloseptin is a unique family of antimicrobial peptides which have been only isolated from frogs of the Phyllomedusinae subfamily. Here, three novel peptide precursors were successfully cloned from a cDNA library, which was constructed from the skin secretion of *Phyllomedusa burmeisteri*, as pair of primers (one NUP and a designed degenerate sense primer) were employed for "shotgun" cloning. The encoded mature peptides were validated by MS/MS sequencing, and subsequently termed as Phylloseptin-PBa1, -PBa2 and -PBa3. Phylloseptin-PBa1 and -PBa2 were demonstrated to possess potent antimicrobial activities against Gram-positive bacteria and yeast, as well as broad-spectrum anticancer activities, while they possess varying haemolytic activity at the effective concentration. In contrast, Phylloseptin-PBa3 was found to exhibit a strong haemolytic activity even though it was only found to possess a weak antimicrobial activity and inconspicuous anticancer activity.

1. Introduction

Antimicrobial peptides (AMPs) are an important participant of the host defence system and play an important role in the innate immunity and the acquired immunity, thus, they also are hailed as the first line of self-defence [1-3]. In the past few decades, through the studies on the self-defense systems ranging from plants to animals, as well as microorganisms, researchers have found that AMPs can be obtained from many organisms [4-10]. Furthermore, because the amphibians are lacking in robust cellular immunity, antimicrobial peptides have become even more important in their host defence system. In the 1960s, investigations on the yellow-bellied toad (*Bombina variegata*), discovered a new family of antimicrobial peptides named "bombinins", which was the first discovery of antimicrobial peptides from frogs with associated haemolytic activity [11]. Hereafter, AMPs from amphibian skin secretion caught increasing attention as a high potential future antibiotic candidate, for their abilities against resistant microorganisms [12].

In the past few years, a series of investigations have been performed on the leaf frogs of the Phyllomedusinae subfamily. These tree frogs inhabit the vast rainforests of Central and South America and have diversified into seven genera and almost sixty species [13]. So far, abundant peptides with antimicrobial activities have been isolated from their skin secretions. Phylloseptins were first isolated from two species of the Phyllomedusa genus (*Phyllomedusa oreades* and *Phyllomedusa hypochondrialis*) and characterised according to their observed antimicrobial activities in 2005 [14]. Subsequent to the initial discovery, phylloseptins were isolated from the skin secretions of many more species from the Phyllomedusinae subfamily [15-20]. There are highly-conserved domains in the signal peptide and acidic spacer peptide domains that are located in the N-terminal regions of all the reported phylloseptins biosynthetic precursors cloned from different species and they generally consist of 15-21 amino acids with similar primary structures. Phylloseptins were reported to have a significant activity against Gram-positive and Gram-negative bacteria and also yeast with an insignificant haemolysis activity at determined MIC concentrations [16.17]. In a

hydrophobic environment or in the membrane, phylloseptins will form into amphiphilic α-helical structures (the polar amino acids, especially the positively-charged lysines and arginines form into the hydrophilic surface, while the non-polar amino acids form into the hydrophobic surface), that might explain their specific recognition of eukaryotic and prokaryotic cell membranes [14.16.19]. In the most recent research, there even reported one phylloseptin peptide was found to have the ability to promote insulin secretion [21].

In this study, "shotgun" cloning procedures were performed and achieved three novel phylloseptin precursor encoding peptides, which were classified as Phylloseptine-PBa1, -PBa2 and -PBa3, from the defensive skin secretion-derived cDNA library of Burmeister's leaf frog (*Phyllomedusa burmeisteri*). The chemically-synthesised peptides were then subjected to antimicrobial, anticancer and haemolysis assays.

2. Material and method

2.1 Specimen biodata and harvest of skin secretion

Adult Burmeister's leaf frog (*phyllomedusa burmeisteri*) (n=4, both sexes, 5-7 cm snout-to-vent length) was obtained from a commercial source and had been captive-bred in the United States. For secretion harvesting, the frogs were bred with multivitamin-loaded cricket feeding three times a week, under artificial controlling conditions with a daily 12 h light exposure at 20-25 ºC for 100 days. Defensive skin secretion was obtained with mild transdermal electrical stimulation (5V, 100Hz, 140ms pulse width) (C.F. Palmer, UK) applied on the dorsal skin surface and flushed with deionised water, then lyophilized and stored at -20 ºC for use. All procedures on living animals were vetted by the IACUC of Queen's University Belfast to approved through the animal experimentation ethics and performed under the guidelines issued by the Department of Health, Social Services and Public Safety, Northern Ireland.

2.2 "Shotgun" Cloning of phylloseptin precursor-encoding cDNA

Polyadenylated mRNA was isolated from the redissolved *P. burmeisteri* skin secretion with Dynabeads mRNA Direct Kits (Thermo Fisher, USA), then subjected to the rapid amplification of cDNA 3'-ends (3'-RACE) procedures, which a nested universal (NUP) primer and a sense primer (5'-ACTTTCYGAWTTRYAAGMCCAAABATG-3') that was designed to a segment of the 5'-untranslated region of phylloxin cDNA from *Phyllomedusa bicolor* (EMBL Accession no. AJ251876) and the opioid peptide cDNA from *Pachymedusa dacnicolor* (EMBL Accession no. AJ005443) were employed to obtain full-length preprophylloseptin nucleic acid sequence data using a SMART-RACE kit (Clontech, UK) essentially as described by the manufacturer. The polymerase chain reaction (PCR) cycling procedure was carried out as follows: Initial denaturation step for 90 s at 94 ºC, 35 cycles of denaturation for 30 s at 94 ºC, primer annealing for 30 s at 58 ºC; extension

for 180 s at 72 ºC. PCR products were subjected to gel-purification and cloning by using a pGEM-T vector system (Promega, USA), then sequenced by using an ABI 3100 Automated Capillary Sequencer (Biosystems, USA).

2.3 Identification and structural analyses of novel phylloseptins in skin secretion

Lyophilised *P. burmeisteri* skin secretion was dissolved in of trifluoroacetic acid (TFA)/water (0.05:99.95, v/v), then injected to an analytical reverse phase HPLC column (Phenomenex C-18, 25 cm × 0.45 cm) and eluted by a gradient formed from 0.05/99.5 (v/v) TFA/water to 0.05/19.95/80.0 (v/v/v) TFA/water/acetonitrile in 240 min at a flow rate of 1 ml/min with fractions were collected automatically at 1 min intervals. Briefly, those fractions were analyzed by using matrix-assisted laser desorption/ionization time-of-flight mass spectrometry (MALDI-TOF MS) (Perseptive Biosystems, MA, USA) in positive detection mode with α-cyano-4-hydroxycinnamic acid as the matrix. The fractions with masses coincident with the calculated molecular masses of predicted novel mature cDNA-encoded phylloseptins were each subjected to primary structural analysis by an LCQ-Fleet electrospray ion-trap mass spectrometer (Thermo Fisher Scientific, USA).

2.4 Solid-phase peptide synthesis of novel phylloseptins and secondary structure prediction

The novel cloned phylloseptins were chemically-synthesised by solid-phase Fmoc chemistry by using a PS3 automated solid-phase synthesiser (Protein Technologies Inc., USA), followed by resin cleavage and side-chain deprotection. As reverse phase HPLC was employed for purification of synthetic peptide purification, the mass spectrometer was applied for structure authentication. The helical wheel projections and relevant physiochemical parameters of peptides, such as the proportion of nonpolar residues, hydrophobicity, hydrophobic moment, and net charge, were achieved by use of Heliquest (http://heliquest.ipmc.cnrs.fr/) [22], while PredictProtein (https://www.predictprotein.org/) [23] was performed for the prediction of the α-helical

proportion and transmembrane domain.

2.5 Antimicrobial assay

The antimicrobial activity of three synthetic novel phylloseptins was evaluated via the minimal inhibitory concentrations (MICs) against three test organisms, a Gram-negative bacteria (*Escherichia coli*, NCTC 10418), a Gram-positive bacteria (*Staphylococcus aureus*, NCTC 10788), and a yeast (*Candida albicans*, NCPF 1467), which were incubated in Mueller-Hinton Broth (MHB). Each phylloseptins were dissolved in dimethylsulfoxide (DMSO) to achieve series of test solutions with concentrations ranging from 1.25 to 160 μM, then added to wells of a 96-well plate, which containing micro-organism suspension with a concentration between 105 and 106 colony forming units (CFU)/mL. Plates were incubated for 24 h at 37°C and then determined by means of measuring optical density (OD) at λ = 550 nm by an ELISA plate reader (Biolise BioTek EL808). Then, a volume of inhibited culture from each well was subcultured on Muller-Hinton Agar (MHA) for another 24 h incubation, the phenomenon with no growth was defined as the minimal bactericidal concentration (MBC).

2.6 Cell Viability of human cancer cells

The synthesized phylloseptins were prepared in concentration of 10^{-5} M for the typical MTT cell viability assay on ten different cancer cell lines: prostate cancer cell lines (DU145, PC3 and LNCaP), lung cancer cell lines (H838, H460, H23 and H157), breast cancer cell lines (MB231, MB435s and MCF-7) and neurospongioma cell line (U251MG). The cancer cell lines, which the testing novel phylloseptins revealed the most significant anticancer activities, was selected for further assay with a range of peptide concentration between 10^{-10} and 10^{-4}. There were two mediums employed in the experiment: Gibco® RPMI-1640 (Invitrogen, USA) for prostate cancer and lung cancer, Dulbecco's Modified Eagle's Medium (DMEM) (Invitrogen, USA) for breast

cancer and neurospongioma. The cell suspensions (in complete medium) of 5×10^3 cells were added to wells of the 96-well plates and incubated for 24 h at 37 °C under 5% CO_2, followed by 12 h incubation with serum-free medium for cell starving. The prepared peptide solutions (in serum-free medium) were added to the wells and incubated for 72 h. A certain amount of MTT solution (5 mg/mL) was added to each well for 6 h of incubation, then the solutions (both MTT and medium) in each well were removed and the precipitated formazan crystals were redissolved in DMSO. The Synergy HT reader (Biotek, USA) was employed to measure the OD value at 550nm.

2.7 Hemolysis assay

The hemolytic activity of each synthetic phylloseptins was determined against 2% prewashed defibrinated horse erythrocytes suspension (TCS Biosciences Ltd., Buckingham, UK). The test peptide solutions were transferred into the aforementioned suspension to prepare a final concentration range from 1.25 to 160 μM and kept at a constant 37°C for 2 h, while odium phosphate-buffered saline and Triton X-100 (Sigma-Aldrich, St. Louis, MO, USA) were employed to replace the peptide solution for establishing the negative and positive control. The supernatants after incubation were measured at 570 nm.

3. Results

3.1 Molecular cloning of Phylloseptin-PBa1, -PBa2, -PBa3 precursor cDNA from a skin secretion-derived cDNA library

Three preprophylloseptin full-length cDNAs were consistently cloned from the *Phyllomedusa burmeisteri* skin secretion-derived cDNA library and each encoded a single copy of a novel mature peptide (Figure 1. A-C), which was constructed by 19 amino acid residues with an amidated C-terminal. The BLASTn (nucleotide/nucleotide) and BLASTp (peptide/peptide) searches performed through the National Center for Biotechnological Information (NCBI) portal revealed that they exhibited high degrees of structural similarity to other reported preprophylloseptin cDNAs and mature phylloseptin peptides. Therefore, these peptides were termed as Phylloseptin-PBa1 (FLSLIPHIASGIASLVKNF-NH_2), Phylloseptin-PBa2 (FLSLLPHIASGIASLVSKF-NH_2) and Phylloseptin-PBa3 (FLSLIPHIVSGVAALANHL-NH_2). AlignX programme of the Vector NTI Bioinformatics suite (Informax, US) was employed for the alignment of these nucleotide sequences (Figure 1. D) and open-reading frame amino acid sequences (Figure 1. E). Both revealed a high degree of similarity between these novel phylloseptins. The cDNA precursors were deposited in GenBank database under an accession no. of MH807621, MH807622, MH807621, respectively.

3.2 Isolation and structural characterisation of Phylloseptin-PBa1, -PBa2, -PBa3

In order to confirm the existence of predicted phylloseptins, which were encoded from the skin secretion-derived cDNA library, RP-HPLC and MS/MS fragmentation sequencing were employed to analyze the *Phyllomedusa burmeisteri* skin secretion. The retention times of these novel phylloseptins were approximately around 120min, and the identities of amino acid sequences have also been verified (Figure 2 and Table 1, respectively).

3.3. Physicochemical properties and secondary structures prediction of Phylloseptin-PBa1, -PBa2, -PBa3

As shown in the wheel projects, K^{17}- Phylloseptin-PBa1 and K^{18}- Phylloseptin-PBa2 were both located in-between hydrophilic and hydrophobic face, as the positively charged C'-terminal of all three phylloseptins were located in the middle of the hydrophobic face (Figure 3. A-C). The predicted secondary structure showed that these phylloseptins exhibited a coil-helix-coil construction (Figure 3. D-F). Because of the peptide C'-terminal amidation and attendance of positively charged amino acid - lysine, both Phylloseptin-PBa1 and -PBa2 have possessed a positive net charge of +2 while Phylloseptin-PBa3 was only positively single charged. The predicted secondary structure composition suggested all three novel phylloseptins presented similar proportion of α-helical domain, which had been deemed to play an important role of antimicrobial mechanism of AMPs, and a similar degree of hydrophobicity and hydrophobic moment while Phylloseptin-PBa3 has one more nonpolar residue than Phylloseptin-PBa1 and -PBa2 (Table 2).

3.4 Antimicrobial activities

Both of Phylloseptin-PBa1 and -PBa2 possessed relatively strong growth inhibitory effects against *S.aureus* and *C.albicans* but exhibited weak activities against *E.coli* (Table 3). MICs of Phylloseptin-PBa1 and -PBa2 were 5 μM, while MBCs were 10 and 5, respectively. MICs of Phylloseptin-PBa1 and -PBa2 for *C.albicans* were 20 and 15μM, respectively, while MBCs were both 20 μM. Meanwhile, Phylloseptin-PBa3 only exhibited weak activities against all three bacterial strains.

3.5 Anticancer activities

Phylloseptin-PBa1, -PBa2 and -PBa3 (concentrations of 10μM) exhibited

intensive anticancer effects on all eleven tested human primary and metastatic cancer cell lines including variety non-small cell lung cancer, breast cancer, prostatic cancer, and neuroglioma (Figure 4. A). Thereinto, Phylloseptin-PBa1 and -PBa2 have demonstrated almost equal activities, while Phylloseptin-PBa3 showed a much weaker capacity. Against the human metastatic breast ductal carcinoma cell line MB435S, which Phylloseptin-PBa1 and -PBa2 showed the most significant anticancer activities, the IC_{50} of Phylloseptin-PBa1, -PBa2 and -PBa3 were 0.29μM, 0.50μM, and 208μM, respectively (Figure 4. B).

3.6 Hemolysis activity

These three phylloseptins exhibited different degrees of hemolytic activities against red blood cells. Nevertheless, Phylloseptin-PBa3 showed a much weaker effect than Phylloseptin-PBa1 and -PBa2, the HC_{50} of Phylloseptin-PBa1, -PBa2 and -PBa3 were 18.60μM, 15.82μM and 53.98μM, respectively (Figure 4. C).

4. Discussions

In recent years, the mode of action of antimicrobial peptides has been studied extensively. Even though the exact mechanism of how such peptides kill microorganisms still needs to be clarified, there is no doubt that peptide-lipid interactions rather than receptor-mediated recognition processes play a key role in the function of most membrane-lytic peptides [24]. AMPs employ some specific steps—attraction, attachment, insertion and membrane permeability to induce killing of bacteria. Though varying greatly in sequences, AMPs generally consist of 12 to 50 amino acids and tend to contain two or more positively-charged amino acids so that they can partition into the bacteria membrane lipid bilayer, which is negatively-charged for their richness of anionic teichoic acids (Gram-positive bacteria) or phospholipids and phosphate groups and teichoic acids (Gram-negative bacteria). [25] Similarly, it goes without saying that the electrostatic attraction between the negatively-charged membranes of cancer cells and AMPs is believed to play an important role in the disruption of cancer cell membranes [26]. Interestingly, many natural AMPs are found to have an amidated C'-terminal that would neutralize the typical C-terminal carboxyl group. There are two possible reasons for this: firstly, peptides will be able to reduce their negative charge that might cause a decrease in their α-helicity; secondly, the increasing of the hydrophobic nature of this region may improve membrane interaction and hence antimicrobial activity [16].

By studying comparatively (Table 4), the antimicrobial activities of reported phylloseptins demonstrated broad-spectrum activities, but the specific antibacterial spectrum of each peptide was different for their unique primary structure. Based on statistics and analysis, it is easy to find out phylloseptins were linear cationic α-helical peptides with a relatively conservative N-terminal domain and a highly variable amidated C-terminal (Table 4). Different from other AMPs, such as brevinins and magainins which contained numerous positively charged amino acids, naturally produced phylloseptins were normally possessed positive net charge less than three with an amidated C-terminal. By comparison, antimicrobial activities of the single

charged phylloseptins were obviously weaker than the double charged phylloseptins while triple charged phylloseptins didn't present significant stronger activities. Recently, a study on the designed cationicity-enhanced phylloseptin analogs showed importation of voluminous lysine (net charge of +6) do not lead to prominent improvement of antimicrobial activities but possible increasing of hemolysis activities [27]. Therefore, lysine located in last three residues of the C-terminal must be playing an important role in phylloseptin's feature. Resende J. M. suggested that the specific lysine was able to create a tilt angle to lifted and moved the C-terminal away from the membrane barrier and dived the N-terminal and α-helical domain into the membrane interior, that developed the function of membrane interface partition and disorder [19]. In addition, some specific amino acid position [20] were also considered to be highly relevant to antimicrobial activities, that might explain the significant activity differences between highly similar Phylloseptin-L1 and Phylloseptin-PLS-S5, Phylloseptin-PTa and Phylloseptin-PC.

This study reports the discovery of three novel phylloseptins from skin secretion of *Phyllomedusa burmeisteri*. As pair of primers (one NUP and a designed degenerate sense primer) were employed for "shotgun" cloning, three preprophylloseptin full-length cDNAs were consistently cloned from the skin secretion-derived cDNA library and each encoded a single copy of a novel mature peptide. The alignment of the three translated open-reading frame amino acid sequences showed highly-conserved signal peptide domains of 22 amino acid residues. The signal peptides of Phylloseptin-PBa2 and -PBa3 were followed by a highly-conserved acidic spacer domain that terminates in a typical –Lys-Arg- (-KR) propeptide convertase processing motif, while the propeptide convertase processing motif of Phylloseptin-PBa1 was –Glu-Arg- (-ER-). All three encoded mature peptides were 19 amino acid residues in length with a C'-terminal amidation. Moreover, the positively charged K^{17}- Phylloseptin-PBa1 and K^{18}-Phylloseptin-PBa2 were both located in between the α-helical domain and random coil domain of C-terminal, which speculated to enhance the activities by creating an insert alignment angle and improving membrane interaction [19]. Therefore, chemosynthetic

Phylloseptin-PBa1 and -PBa2 exhibited weak activities against Gram-negative bacteria and potent effects on Gram-positive bacteria (MICs of 5 μM) and the yeast (MICs of 20 μM and 15 μM), while Phylloseptin-PBa3 was found to have no prominent effect on all three test organisms. Similarly, as Phylloseptin-PBa1 and -PBa2 demonstrated the most significant activities against metastatic ductal adenocarcinoma of the breast (MB435s), Phylloseptin-PBa3 presented comparatively weaker anticancer activities over all tested cancer cell lines. Furthermore, Phylloseptin-PBa1 and -PBa2 possessed no obvious hemolytic activity at the MICs against Gram-positive bacteria, which greatly increased the potential for future clinical drug development.

In conclusion, these studies clarified a method to identify novel naturally produced bioactive peptides from amphibian skin secretion, and also provide valuable clues for the design of analogs with higher activities and lower biological hazard, which might lead to an evolution of anti-infective and anti-tumor drug.

Acknowledgments

This work was supported by Natural Science Foundation of Fujian Province of China (Youth Innovation) [grant number 2015J05158]; Miaopu Science Research Foundation of Fujian Medical University [grant number 2014MP009].

Reference

[1] Erspamer V. Bioactive secretions of the amphibian integument[J]. *Amphibian biology*, 1994, 1: 178-350.

[2] Bevins C L, Zasloff M. Peptides from frog skin[J]. *Annual review of biochemistry*, 1990, 59(1): 395-414.

[3] Clarke B T. The natural history of amphibian skin secretions, their normal functioning and potential medical applications[J]. *Biological Reviews*, 1997, 72(3): 365-379.

[4] Reddy K V R, Yedery R D, Aranha C. Antimicrobial peptides: premises and promises[J]. *International journal of antimicrobial agents*, 2004, 24(6): 536-547.

[5] Hannah Farkas H. Bacteriocins—are they broad-spectrum antibiotics?[J]. *Journal of Antimicrobial Chemotherapy*, 1980, 6(4): 424-427.

[6] Lauwers A, Twyffels L, Soin R, et al. Post-transcriptional regulation of genes encoding anti-microbial peptides in Drosophila[J]. Journal of Biological Chemistry, 2009, 284(13): 8973.

[7] Cole A M, Weis P, Diamond G. Isolation and characterization of pleurocidin, an antimicrobial peptide in the skin secretions of winter flounder[J]. *Journal of Biological Chemistry*, 1997, 272(18): 12008-12013.

[8] Marenah L, Flatt P R, Orr D F, et al. Brevinin-1 and multiple insulin-releasing peptides in the skin of the frog *Rana palustris*[J]. *Journal of endocrinology*, 2004, 181(2): 347-354.

[9] White S H, Wimley W C, Selsted M E. Structure, function, and membrane integration of defensins[J]. *Current opinion in structural biology*, 1995, 5(4): 521-527.

[10] Florack D E A, Stiekema W J. Thionins: properties, possible biological roles and mechanisms of action[J]. *Plant molecular biology*, 1994, 26(1): 25-37.

[11] Kiss G, Michl H. On the venomous skin secretion of the orange speckled frog

Bombina variegata[J]. *Toxicon*, 1962, 1: 33-39.

[12] Antosova Z, Mackova M, Kral V, et al. Therapeutic application of peptides and proteins: parenteral forever?[J]. *Trends in biotechnology*, 2009, 27(11): 628-635.

[13] Frost D, Grant T, Faivovich J, et al. The amphibian tree of life[J]. *Bulletin of the American Museum of natural History*, 2006, 297(297):1-291.

[14] Leite J R S A, Silva L P, Rodrigues M I S, et al. Phylloseptins: a novel class of anti-bacterial and anti-protozoan peptides from the *Phyllomedusa* genus[J]. *Peptides*, 2005, 26(4): 565-573.

[15] Conceicao K, Konno K, Richardson M, et al. Isolation and biochemical characterization of peptides presenting antimicrobial activity from the skin of *Phyllomedusa hypochondrialis*[J]. *Peptides*, 2006, 27(12): 3092-3099.

[16] Resende J M, Moraes C M, Prates M V, et al. Solution NMR structures of the antimicrobial peptides phylloseptin-1,-2, and-3 and biological activity: the role of charges and hydrogen bonding interactions in stabilizing helix conformations[J]. *Peptides*, 2008, 29(10): 1633-1644.

[17] Zhang R, Zhou M, Wang L, et al. Phylloseptin-1 (PSN-1) from *Phyllomedusa sauvagei* skin secretion: a novel broad-spectrum antimicrobial peptide with antibiofilm activity[J]. *Molecular immunology*, 2010, 47(11-12): 2030-2037.

[18] König E, Clark V C, Shaw C, et al. Molecular cloning of skin peptide precursor-encoding cDNAs from tibial gland secretion of the Giant Monkey Frog, *Phyllomedusa bicolor* (Hylidae, Anura)[J]. *Peptides*, 2012, 38(2): 371-376.

[19] Resende J M, Verly R M, Aisenbrey C, et al. Membrane interactions of phylloseptin-1,-2, and-3 peptides by oriented solid-state NMR spectroscopy[J]. *Biophysical journal*, 2014, 107(4): 901-911.

[20] Wu X, Pan J, Wu Y, et al. PSN-PC: A Novel Antimicrobial and Anti-Biofilm Peptide from the Skin Secretion of *Phyllomedusa-camba* with Cytotoxicity on Human Lung Cancer Cell[J]. *Molecules*, 2017, 22(11): 1896.

[21] Long Q, Wang L, Zhou M, et al. A novel peptide Phylloseptin-PBu from *Phyllomedusa burmeisteri* possesses insulinotropic activity via potassium channel and GLP-1 receptor signalling[J]. *Journal of cellular and molecular medicine*, 2018, 22(5): 2804-2814.

[22] Gautier R, Douguet D, Antonny B, et al. HELIQUEST: a web server to screen sequences with specific α-helical properties[J]. *Bioinformatics*, 2008, 24(18): 2101-2102.

[23] Rost B, Yachdav G, Liu J. The predictprotein server[J]. *Nucleic acids research*, 2004, 32(suppl_2): W321-W326.

[24] Shai Y. Mechanism of the binding, insertion and destabilization of phospholipid bilayer membranes by α-helical antimicrobial and cell non-selective membrane-lytic peptides[J]. *Biochimica et Biophysica Acta (BBA)-Biomembranes*, 1999, 1462(1-2): 55-70.

[25] Brogden K A. Antimicrobial peptides: pore formers or metabolic inhibitors in bacteria?[J]. *Nature reviews microbiology*, 2005, 3(3): 238.

[26] Schweizer F. Cationic amphiphilic peptides with cancer-selective toxicity[J]. *European journal of pharmacology*, 2009, 625(1-3): 190-194.

[27] Gao Y, Wu D, Xi X, et al. Identification and characterisation of the antimicrobial peptide, phylloseptin-PT, from the skin secretion of Phyllomedusa tarsius, and comparison of activity with designed, cationicity-enhanced analogues and diastereomers[J]. *Molecules*, 2016, 21(12): 1667.

[28] Chen T, Zhou M, Gagliardo R, et al. Elements of the granular gland peptidome and transcriptome persist in air-dried skin of the South American orange-legged leaf frog, *Phyllomedusa hypocondrialis*[J]. *Peptides*, 2006, 27(9): 2129-2136.

[29] Conlon J M, Woodhams D C, Raza H, et al. Peptides with differential cytolytic activity from skin secretions of the lemur leaf frog *Hylomantis lemur* (Hylidae: Phyllomedusinae)[J]. *Toxicon*, 2007, 50(4): 498-506.

[30] Raja Z, Andre S, Piesse C, et al. Structure, antimicrobial activities and mode of interaction with membranes of bovel phylloseptins from the painted-belly leaf frog, *phyllomedusa sauvagii*[J]. *PLoS One*, 2013, 8(8): e70782.

[31] Wan Y, Ma C, Zhou M, et al. Phylloseptin-PBa—A novel broad-spectrum antimicrobial peptide from the skin secretion of the peruvian purple-sided leaf frog (*phyllomedusa baltea*) which exhibits cancer cell cytotoxicity[J]. *Toxins*, 2015, 7(12): 5182-5193.

[32] Yang N, Li L, Wu D, et al. Discovery of novel bacterial cell-penetrating phylloseptins in defensive skin secretions of the south american hylid frogs, *phyllomedusa duellmani* and *phyllomedusa coelestis*[J]. *Toxins*, 2016, 8(9): 255.

[33] Liu J, Wu Q, Li L, et al. Discovery of phylloseptins that defense against gram-positive bacteria and inhibit the proliferation of the non-small cell lung cancer cell line, from the skin secretions of Phyllomedusa frogs[J]. *Molecules*, 2017, 22(9): 1428.

Legends to Figures and Tables

Figure 1. Nucleotide sequences of cloned cDNA encoding the biosynthetic precursor of Phylloseptin-PBa1 **(a)**, -PBa2 **(b)** and -PBa3 **(c)** translated amino acid sequences of the open reading frame. Putative signal peptides are double-underlined, mature peptides are single-underlined and the stop codons are indicated by asterisks. **(d)** Alignment of nucleotide sequences of phylloseptin precursor cDNAs cloned from the *P. burmeisteri* skin secretion-derived cDNA library. **(e)** Alignment of translated open-reading frame amino acid sequences of *P. burmeisteri* phylloseptin precursors deduced from cloned cDNAs. Identical bases in all three are shaded in yellow. Consensus bases in two sequences are shaded blue. Gaps have been inserted to maximise alignments.

Figure 2. Region of RP–HPLC chromatogram of *Phyllomedusa burmeisteri* skin secretion indicating the absorbance peaks by arrows that corresponds to Phylloseptin-PBa1, -PBa2 and -PBa3.

Figure 3. Predicted helical wheel projections of Phylloseptin-PBa1**(a)**, -PBa2**(b)** and -PBa3**(c)**. Predicted secondary structure of Phylloseptin-PBa1**(d)**, -PBa2**(e)** and -PBa3**(f)** (H: helix, L:coil).

Figure 4. Bioactive activities of Phylloseptin-PBa1, -PBa2, -PBa3 **(a)** Cell viability against different cancer cell lines treated with phylloseptins with concentration of 10^{-5} M. **(b)** The cytotoxic effect of phylloseptins on the human metastatic breast ductal carcinoma cell line MB435S. **(c)** Haemolytic activity of Phylloseptins against horse red blood cells.

Table 1. Electrospray ion-trap MS/MS fragmentation sequencing datasets derived from ions corresponding in molecular mass to Phylloseptin-PBa1 **(a)**, -PBa2 **(b)** and -PBa3 **(c)**. Expected singly- and doubly-charged b-ion and y-ion fragment m/z ratios were predicted using the MS-Product programme available through Protein Prospector on-line. Observed ions are shown in red and blue.

Table 2. Physicochemical of Phylloseptin-PBa1, -PBa2, -PBa3.

Table 3. Antimicrobial activity of Phylloseptin-PBa1, -PBa2, -PBa3 against various microorganisms.

Table 4. Minimum inhibitory concentrations (MICs) and physicochemical parameters of natural phylloseptins against specified microorganisms.

```
      M  A  F  L  K  K  S  L  F  L  V  L  F  F  G  L  V  ·
  1   ATGGCTTTCT TGAAGAAATC GCTTTTCCTT GTACTATTCT TTGGATTGGT
      ·  S  L  S  I  C  E  E  E  K  R  E  T  E  E  E  E  H  ·
 51   TTCCCTTTCC ATCTGTGAAG AAGAGAAAAG AGAGACTGAA GAGGAAGAAC
      ·  D  Q  E  E  D  D  K  S  E  E  E  R  F  L  S  L
101   ATGATCAAGA GGAAGATGAT AAAAGTGAAG AGGAGAGATT CTTGAGCTTG
       I  P  H  I  A  S  G  I  A  S  L  V  K  N  F  G  *  ·
151   ATACCACATA TTGCATCTGG AATAGCTTCA CTTGTTAAAA ACTTCGGTTA
      ·  *
201   ATACAATGTA ACATTTCATA ACTCTAAGGA GCACAATTAT CAATAATTGT
251   TCTCAAAATA CATTAAAGCA TATTTAACAA AAAAAAAAAA AAAAAAAAAA
```

(A)

```
      M  A  F  L  K  K  S  L  F  L  V  L  F  L  G  L  V  ·
  1   ATGGCTTTCT TGAAAAAATC TCTTTTCCTT GTACTATTCC TTGGATTGGT
      ·  S  L  S  I  C  E  E  E  K  R  E  T  E  E  E  E  H  ·
 51   TTCCCTTTCC ATCTGTGAAG AAGAGAAAAG AGAGACTGAA GAGGAAGAAC
      ·  D  Q  E  E  D  D  K  S  E  E  K  R  F  L  S  L
101   ATGATCAAGA GGAAGATGAT AAAAGTGAAG AGAAGAGATT CTTGAGCTTG
       L  P  H  I  A  S  G  I  A  S  L  V  S  K  F  G  *  ·
151   TTACCACATA TAGCATCTGG AATAGCTTCA CTCGTTTCAA AATTCGGTTA
      ·  *
201   ATACAATGTG TAATTACATA ACTCTAAGGA GCACAATTAT CAATAATTGT
251   CCTCAAAATA CATTAAAGCA TATTTAACCA AAAGAAAAAA AAAAAAAAAA
301   AAAAAAAAAA
```

(B)

```
      M  A  F  L  K  K  S  L  F  L  V  L  F  L  G  L  V  ·
  1   ATGGCTTTCT TGAAAAAATC TCTATTCCTT GTACTTTTCC TTGGATTGGT
      ·  S  L  S  I  C  E  K  K  K  R  E  T  E  E  E  E  H  ·
 51   TTCCCTTTCT ATCTGTGAAA AAAAAAAAAG GGAGACTGAA GAGGAAGAAC
      ·  D  Q  E  E  D  D  K  S  E  K  K  R  F  L  S  L
101   ATGATCAAGA GGAAGATGAT AAAAGTGAAA AGAAAAGATT CCTCAGCTTG
       I  P  H  I  V  S  G  V  A  A  L  A  N  H  L  G  *  ·
151   ATACCACATA TCGTATCTGG AGTAGCTGCA CTTGCTAACC ATTTAGGTTA
      ·  *
201   ATACAATGTA ACATTTCATA ACTCTAAGGA GCACAATTAT CAATAATTGT
251   CCTCAAAATA CATTAAAGCA TATTTAACAA AAAAAAAAAA AAAAAAAAAA
```

(C)

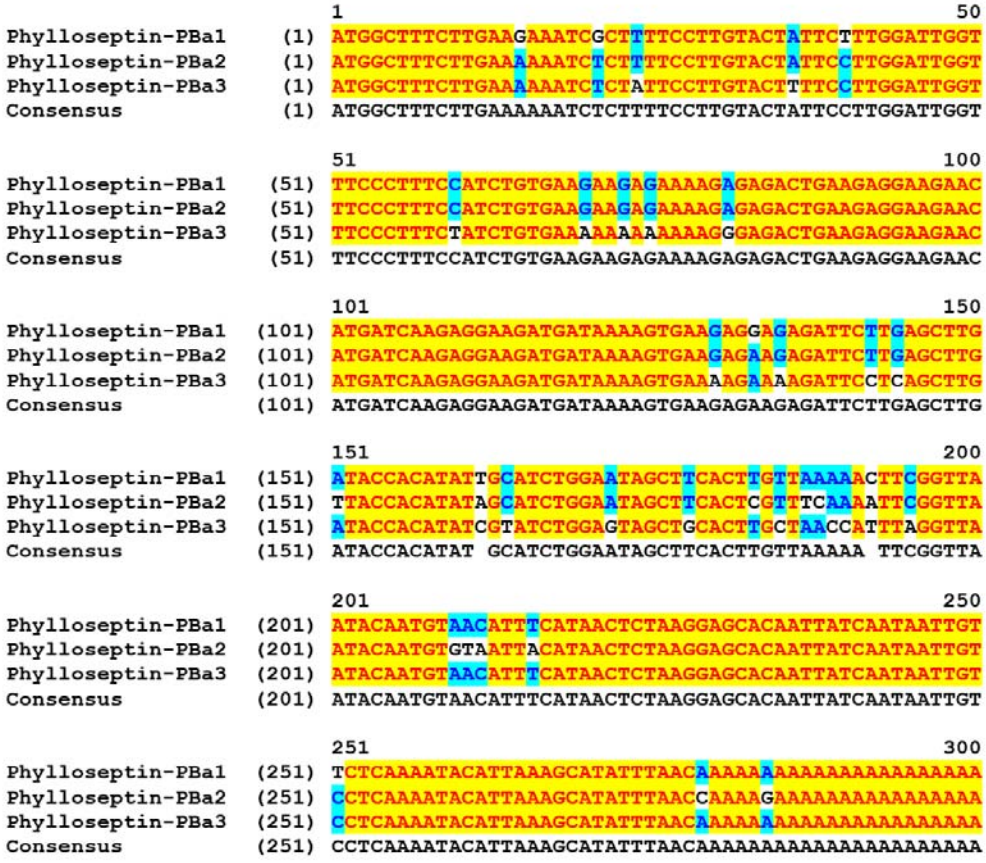

(D)

(E)

Figure 1. Nucleotide sequences of cloned cDNA encoding the biosynthetic precursor of Phylloseptin-PBa1 **(A)**, -PBa2 **(B)** and -PBa3 **(C)** translated amino acid sequences of the open reading frame. Putative signal peptides are double-underlined, mature peptides are single-underlined and the stop codons are indicated by asterisks. **(D)** Alignment of nucleotide sequences of phylloseptin precursor cDNAs cloned from the *P. burmeisteri* skin secretion-derived cDNA library. **(E)** Alignment of translated open-reading frame amino acid sequences of *P. burmeisteri* phylloseptin precursors deduced from cloned cDNAs. Identical bases in all three are shaded in yellow. Consensus bases in two sequences are shaded blue. Gaps have been inserted to maximise alignments.

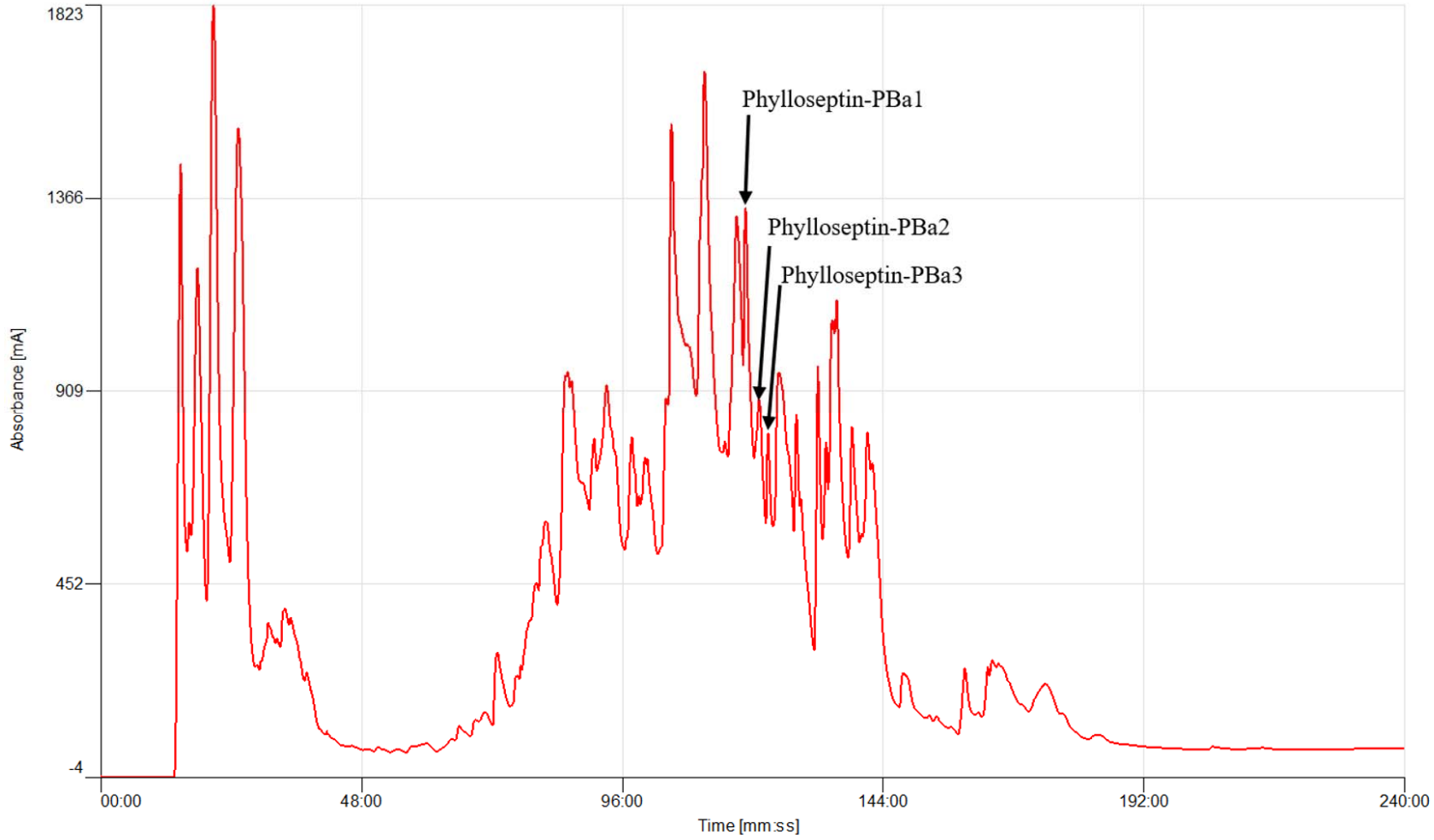

Figure 2. Region of RP–HPLC chromatogram of *Phyllomedusa burmeisteri* skin secretion indicating the absorbance peaks by arrows that corresponds to Phylloseptin-PBa1, -PBa2 and -PBa3.

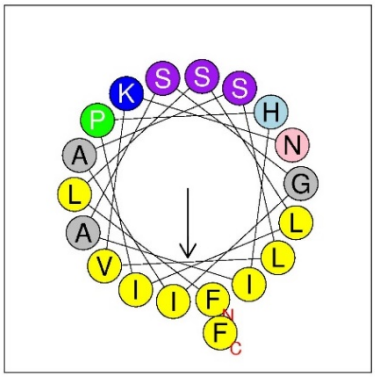

(A)

```
                ....,....1....,....2
AA              FLSLIPHIASGIASLVKNF
OBS_sec
PROF_sec          HHHHHHHHHHHHHH
Rel_sec         901126778679888741 8
SUB_sec         L....HHHHHHHHHH..L
```

(D)

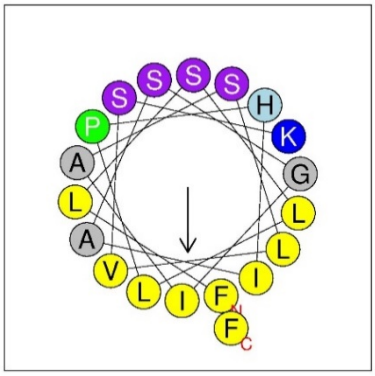

(B)

```
                ....,....1....,....2
AA              FLSLLPHIASGIASLVSKF
OBS_sec
PROF_sec          HHHHHHHHHHHHHH
Rel_sec         911347778668877630 8
SUB_sec         L....HHHHHHHHHH..L
```

(E)

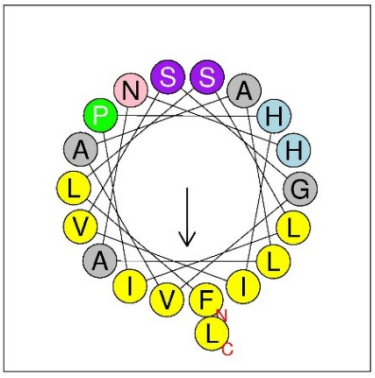

(C)

```
                ....,....1....,....2
AA              FLSLIPHIVSGVAALANHL
OBS_sec
PROF_sec          HHHHHHHHHHHHHHH
Rel_sec         800224578889888720 8
SUB_sec         L.....HHHHHHHHH..L
```

(F)

Figure 3. Predicted helical wheel projections of Phylloseptin-PBa1**(A)**, -PBa2**(B)** and -PBa3**(C)**. Predicted secondary structure of Phylloseptin-PBa1**(D)**, -PBa2**(E)** and -PBa3**(F)** (H: helix, L:coil).

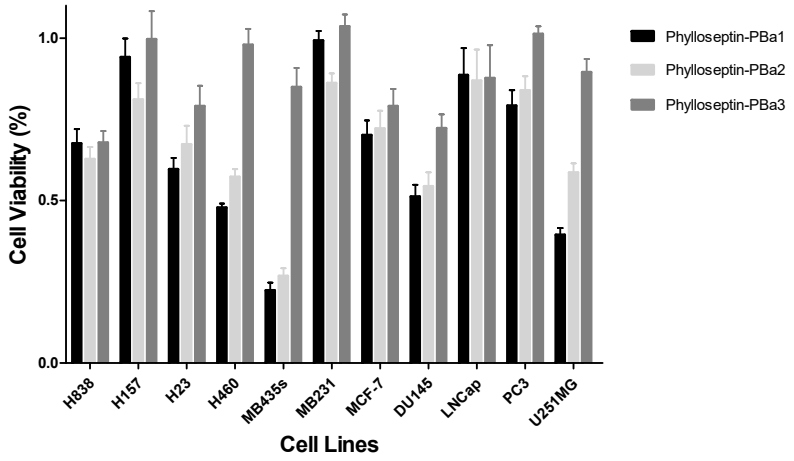

(A)

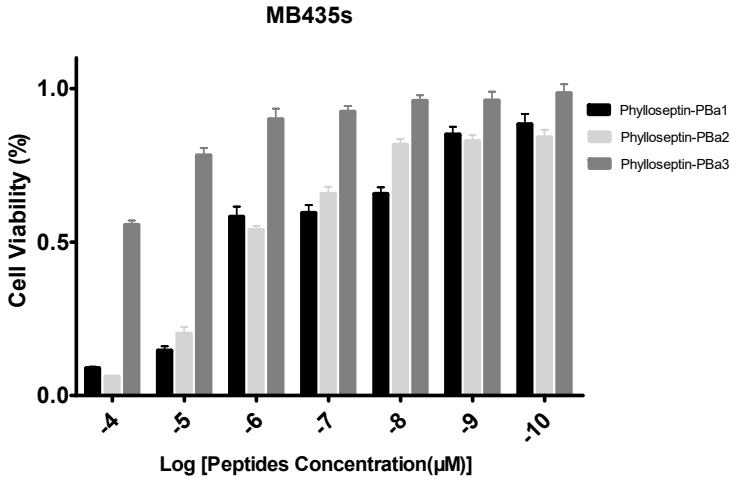

(B)

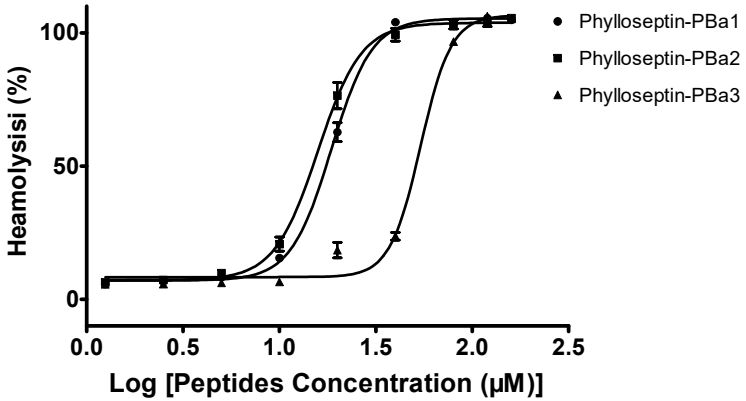

(C)

Figure 4. Bioactive activities of Phylloseptin-PBa1, -PBa2, -PBa3 **(A)** Cell viability against different cancer cell lines treated with phylloseptins with concentration of 10^{-5} M. **(B)** The cytotoxic effect of phylloseptins on the human metastatic breast ductal carcinoma cell line MB435S. **(C)** Haemolytic activity of Phylloseptins against horse red blood cells.

Table 1. Electrospray ion-trap MS/MS fragmentation sequencing datasets derived from ions corresponding in molecular mass to Phylloseptin-PBa1 **(A)**, -PBa2 **(B)** and -PBa3 **(C)**. Expected singly- and doubly-charged b-ion and y-ion fragment m/z ratios were predicted using the MS-Product programme available through Protein Prospector on-line. Observed ions are shown in red and blue.

#1	b(1+)	b(2+)	Seq.	y(1+)	y(2+)	#2
1	148.07570	74.54149	F			19
2	261.15977	131.08352	L	1879.11647	940.06187	18
3	348.19180	174.59954	S	1766.03240	883.51984	17
4	461.27587	231.14157	L	1679.00037	840.00382	16
5	574.35994	287.68361	I	1565.91630	783.46179	15
6	671.41271	336.20999	P	1452.83223	726.91975	14
7	808.47162	404.73945	H	1355.77946	678.39337	13
8	921.55569	461.28148	I	1218.72055	609.86391	12
9	992.59281	496.80004	A	1105.63648	553.32188	11
10	1079.62484	540.31606	S	1034.59936	517.80332	10
11	1136.64631	568.82679	G	947.56733	474.28730	9
12	1249.73038	625.36883	I	890.54586	445.77657	8
13	1320.76750	660.88739	A	777.46179	389.23453	7
14	1407.79953	704.40340	S	706.42467	353.71597	6
15	1520.88360	760.94544	L	619.39264	310.19996	5
16	1619.95202	810.47965	V	506.30857	253.65792	4
17	1748.04699	874.52713	K	407.24015	204.12371	3
18	1862.08992	931.54860	N	279.14518	140.07623	2
19			F-Amidated	165.10225	83.05476	1

(A)

#1	b(1+)	b(2+)	Seq.	y(1+)	y(2+)	#2
1	148.07570	74.54149	F			19
2	261.15977	131.08352	L	1852.10557	926.55642	18
3	348.19180	174.59954	S	1739.02150	870.01439	17
4	461.27587	231.14157	L	1651.98947	826.49837	16
5	574.35994	287.68361	L	1538.90540	769.95634	15
6	671.41271	336.20999	P	1425.82133	713.41430	14
7	808.47162	404.73945	H	1328.76856	664.88792	13
8	921.55569	461.28148	I	1191.70965	596.35846	12
9	992.59281	496.80004	A	1078.62558	539.81643	11
10	1079.62484	540.31606	S	1007.58846	504.29787	10
11	1136.64631	568.82679	G	920.55643	460.78185	9
12	1249.73038	625.36883	I	863.53496	432.27112	8
13	1320.76750	660.88739	A	750.45089	375.72908	7
14	1407.79953	704.40340	S	679.41377	340.21052	6
15	1520.88360	760.94544	L	592.38174	296.69451	5
16	1619.95202	810.47965	V	479.29767	240.15247	4
17	1706.98405	853.99566	S	380.22925	190.61826	3
18	1835.07902	918.04315	K	293.19722	147.10225	2
19			F-Amidated	165.10225	83.05476	1

(B)

#1	b(1+)	b(2+)	Seq.	y(1+)	y(2+)	#2
1	148.07570	74.54149	F			19
2	261.15977	131.08352	L	1824.08550	912.54639	18
3	348.19180	174.59954	S	1711.00143	856.00435	17
4	461.27587	231.14157	L	1623.96940	812.48834	16
5	574.35994	287.68361	I	1510.88533	755.94630	15
6	671.41271	336.20999	P	1397.80126	699.40427	14
7	808.47162	404.73945	H	1300.74849	650.87788	13
8	921.55569	461.28148	I	1163.68958	582.34843	12
9	1020.62411	510.81569	V	1050.60551	525.80639	11
10	1107.65614	554.33171	S	951.53709	476.27218	10
11	1164.67761	582.84244	G	864.50506	432.75617	9
12	1263.74603	632.37665	V	807.48359	404.24543	8
13	1334.78315	667.89521	A	708.41517	354.71122	7
14	1405.82027	703.41377	A	637.37805	319.19266	6
15	1518.90434	759.95581	L	566.34093	283.67410	5
16	1589.94146	795.47437	A	453.25686	227.13207	4
17	1703.98439	852.49583	N	382.21974	191.61351	3
18	1841.04330	921.02529	H	268.17681	134.59204	2
19			L-Amidated	131.11790	66.06259	1

(C)

Table 2. Physicochemical of Phylloseptin-PBa1, -PBa2, -PBa3

Peptide	% Helix	Nonpolar Residues (n/%)	Hydrophobicity <H>	Hydrophobic Moment <μH>	Net Charge
Phylloseptin-PBa1	73.68%	12/63.16%	0.793	0.606	+2
Phylloseptin-PBa2	73.68%	12/63.16%	0.817	0.569	+2
Phylloseptin-PBa3	78.95%	13/68.42%	0.835	0.509	+1

Table 3. Antimicrobial activity of Phylloseptin-PBa1, -PBa2, -PBa3 against various microorganisms.

Peptiedes	MIC (μM)			MBC (μM)		
	S. aureus	*E. coli*	*C. albicans*	*S. aureus*	*E. coli*	*C. albicans*
Phylloseptin-PBa1	5	200	20	10	>200	20
Phylloseptin-PBa2	5	200	15	5	>200	20
Phylloseptin-PBa3	>200	>200	200	>200	>200	>200

Table 4. Minimum inhibitory concentrations (MICs) and physicochemical parameters of natural phylloseptins against specified microorganisms.

Peptide name	Sequence	MIC (μM)			Net Charge	Hydrophobicity <H>	% Helix	Reference
		E. coli	*S. aureus*	*C. albicans*				
Phylloseptin-PBa1	FLSLIPHIASGIASLVKNF-NH_2	200	5	20	+2	0.793	73.68%	
Phylloseptin-PBa2	FLSLLPHIASGIASLVSKF-NH_2	200	5	15	+2	0.817	73.68%	
Phylloseptin-PBa3	FLSLIPHIVSGVAALANHL-NH_2	>200	>200	200	+1	0.835	78.95%	
Phylloseptin-1	FLSLIPHAINAVSAIAKHN-NH_2	7.9	7.9	ND	+2	0.619	89.47%	[14]
Phylloseptin-7	FLSLIPHAINAVSAIAKHF-NH_2	100	100	ND	+2	0.745	89.47	[15.28]
phylloseptin-L1	LLGMIPLAISAISALSKL-NH_2	>128	8	ND	+2	0.871	77.78%	[29]
Phylloseptin-PSN1	FLSLIPHIVSGVASIAKHF-NH_2	80	5	100	+2	0.806	68.42%	[17]
Phylloseptin-PLS-S2	FLSLIPHIVSGVASLAKHF-NH_2	25	6.25	ND	+2	0.801	78.95%	[30]
Phylloseptin-PLS-S3	FLSLIPHIVSGVASLAIHF-NH_2	>200	>200	ND	+1	0.947	73.68%	
Phylloseptin-PLS-S4	FLSMIPHIVSGVAALAKHL-NH_2	25	6.25	ND	+2	0.789	78.95%	
Phylloseptin-PLS-S5	LLGMIPVAISAISALSKL-NH_2	>100	>200	ND	+2	0.844	72.22%	
Phylloseptin-PBa	FFSMIPKIAGGIASLVKNL-NH_2	128	8	8	+3	0.711	73.68%	[31]
Phylloseptin-Du	FFSMIPKIATGIASLVKNL-NH_2	62	4	8	+3	0.725	68.42%	[32]
Phylloseptin-Co	FLSMIPKIAGGIASLVKNL-NH_2	65	4	8	+3	0.706	73.68%	
Phylloseptin-PTa	FLSLIPKIAGGIAALAKHL-NH_2	17	4	2	+3	0.740	89.47%	[33]
Phylloseptin-Pha	FLSLIPAAISAVSALANH-NH_2	>264	33	132	+1	0.744	83.33%	
Phylloseptin-PC	FLSLIPKIATGIAALAKHL-NH_2	8	2	2	+3	0.754	89.47%	[20]

ND: not detected. Physicochemical parameters were predicted by online analysis tool HeliQuest and PredictProtein.